Mathematics

https://www.aimspress.com/journal/Math

AIMS Mathematics, 11(9): 28436–28451.
DOI: 10.3934/math.20261132
Received: 14 June 2026
Revised: 12 August 2026
Accepted: 24 August 2026
Published: 04 September 2026

Research article

Design of distributed interval observer for cyber-physical system

Danxia Li[1,*], Shan Wang[1], Yujie Chu[1], Qian Shen[1], Jiale Mi[1] and Zipeng Wang[2]

[1] School of Intelligent Engineering, Henan Institute of Technology, Xinxiang 453007, China
[2] School of Information Science and Technology, Beijing University of Technology, Beijing 100124, China

* **Correspondence:** Email: danxia_li@163.com.

Abstract: Cyber-physical systems (CPS) possess the characteristics of distribution and heterogeneity. The states of each subsystem are interrelated, and the information is dispersed. A single observer can only obtain partial measurement information and is unable to estimate all the states of the system. In this paper, a distributed interval observer (DIO) design method is proposed for CPS with bounded uncertainties and affected by disturbances and noise. Compared with traditional interval observers, it no longer requires the original system to be cooperative or the estimation error system to have an order-preserving property. This broadens the application scope of distributed interval observers. Sufficient conditions for the bounded stability of the observer error system are given using Lyapunov stability theory and Riccati equation. Finally, numerical simulations prove the effectiveness of the proposed method.

Keywords: distributed interval observer; cyber-physical system; bounded uncertainty; state estimation
Mathematics Subject Classification: 93B07, 93B53, 93C05, 93D05

1. Introduction

With the deep integration of industrial intelligence and Internet of things technology, cyber-physical systems (CPS) have become the core support in the fields of intelligent manufacturing and various industrial energy scenarios [1, 2]. In practical scenarios, sensor deployment can only obtain partial output information due to cost and space constraints [3]. Centralized estimation has inherent defects. To break through this technical bottleneck, distributed observers are widely used. It has excellent scalability and robustness and has become the mainstream technology of state estimation in CPS. Its core design idea is to decompose the global state estimation task into local estimation and limited information interaction between nodes and to offset the information limitations of a single observation point through node cooperation [4]. This aligns with the essential characteristics of distributed operation in CPS. In recent years, the research on observer technology of distributed state estimation has attracted much attention and has achieved many results: Aiming at the problem of cooperative output regulation of heterogeneous multi-agents under uncertain external systems, Zhang [3] designed an output-based distributed adaptive observer. The estimation of external system parameters and state index is realized. For the distributed state estimation problem of unknown input linear time-invariant (LTI) systems, Long [5] proposed an adaptive event-triggered distributed observer.

However, in practical engineering applications, due to the existence of uncertainties such as disturbance and noise, it is difficult to achieve accurate estimation of the system state, or the implementation cost is very high. Therefore, it is necessary to develop a low-cost interval estimation scheme. Therefore, Gouzé et al. first proposed the interval observer technique [6]. Interval observer has become a research hotspot in the field of control theory and engineering. Many achievements have been made in performance improvement, application scope expansion, and structural innovation: Mazenc et al. [7] proposed an exponentially stable interval observer design method for LTI with disturbances. Wang et al. [8] extended the interval observer to linear singular systems. Zhu et al. [9] further focused on linear discrete switched systems, and regarded bounded disturbance and measurement noise as augmented state variables combined with a multi-Lyapunov function method to achieve accurate interval estimation. Meslem et al. [10] proposed a new structure of the interval observer for continuous-time linear systems, which breaks through the structural limitations of the classical Luenberger observer. Zhang et al. [11] applied the interval observer to the CPS attack detection scenario, which strengthened the engineering practicability of the interval observer.

Although interval observers and distributed observers have made some progress, the research on the distributed interval observer (DIO) with deep integration of the two is still in its infancy [12]. In recent years, a number of technical paths have gradually emerged in the design of the DIO: By combining the interior positive representation (IPR) with the synchronous region method, the DIO is constructed to ensure that the error system is stable and positive definite [12]. The system is detected and decomposed, and only the IPR technology is applied to the undetectable subsystem of the system. A fully reduced-order DIO for LTI systems with disturbance and measurement noise is constructed [13]. By updating the local inter-regional estimation interaction and intersection operation between agents, the necessary and sufficient conditions of collective stability and the distributed construction method are given. For nonlinear discrete-time multi-agent systems, under the challenge of unknown or bounded adversarial input, a complete framework for distributed elastic interval observer design and stability analysis is proposed [14]. In addition, the DIO is also deeply integrated with the event-triggered mechanism, which provides a controller design method for the network LTI system [15]. For multi-Eulerian-Lagrange systems, the DIO designed by coordinate transformation and monotone system theory improves the adaptability [16]. Although the DIO has achieved some results, it still has obvious limitations such as large amount of calculation [13] and narrow application range [12, 14–16]. Inspired by the above discussion, this paper proposes a new DIO design method for the CPS. The main contributions are as follows:

(1) Compared with Reference [9], this scheme introduces a distributed architecture, which can estimate the upper and lower bounds of the system state in real time, and is suitable for scenarios with non-high-precision observation requirements, effectively reducing the observation cost.

(2) In the design of the DIO, it is important to keep the order of the error system. In order

to overcome this difficulty, References [12, 13] used the IPR method to increase the dimension of the system, while Reference [15] required that the original system matrix can be transformed into Metzler matrix form, but this paper does not need this restriction. In this paper, the system matrix is decomposed into the form of the difference between the Metzler matrix and the nonnegative matrix, which no longer depends on the IPR dimension, and does not need to limit the system matrix to a positive matrix or Metzler matrix, thus effectively reducing the computational complexity and broadening the application scenario.

Preliminaries on graph theory and notation: Distributed interaction depends on the communication topology between nodes, which is described by a directed graph $\mathcal{G} = (\mathcal{V}, \mathcal{E}, \mathcal{A})$: $\mathcal{V} = \{1, 2, \ldots, N\}$ is the set of nodes; $\mathcal{E} \subseteq \mathcal{V} \times \mathcal{V}$ is the edge set, where $(i, k) \in \mathcal{E}$ denotes that nodes i and k can communicate directly; $\mathcal{A} = [a_{ik}] \in \mathbb{R}^{N\times N}$ represents the adjacency matrix with $a_{ik} = 1$ if and only if $(i, k) \in \mathcal{E}$, otherwise $a_{ik} = 0$; and the neighborhood set of node i is defined as $N_i = \{j \mid (i, j) \in \mathcal{E}\}$. For a matrix P, P^T, and P^{-1}, denote its transpose and its inverse, respectively. Furthermore, the Metzler representation of P is denoted by $P^{\mathcal{M}}$ and given by $P^{\mathcal{M}} = \begin{bmatrix} \mathcal{D}_P + \mathcal{F}_P^+ & \mathcal{F}_P^- \\ \mathcal{F}_P & \mathcal{D}_P + \mathcal{F}_P^+ \end{bmatrix}$. $P^{\mathcal{M}}$ is a Metzler representation of matrix P, where $\mathcal{D}_P = \mathrm{diag}\{p_{11}, \ldots, p_{nn}\}$ and $\mathcal{F}_P = P - \mathcal{D}_P$, $\mathcal{F}_P^+$ and $\mathcal{F}_P^-$ are the elementwise positive and negative parts of $\mathcal{F}_P$, respectively, defined by $\mathcal{F}_P^+ = \max\{\mathcal{F}_P, 0\}, \mathcal{F}_P^- = \max\{-\mathcal{F}_P, 0\}$. Consequently, $\mathcal{F}_P = \mathcal{F}_P^+ - \mathcal{F}_P^-$, and both $\mathcal{F}_P^+$ and $\mathcal{F}_P^-$ are nonnegative elementwise. I denotes the identity matrix with appropriate dimension, and $\mathbf{0}$ denotes the null matrix of suitable dimensions. $\otimes$ represents the Kronecker product, $\|x\|$ denotes the Euclidean norm of x, and $|\mathcal{V}|$ denotes the cardinality of the set $\mathcal{V}$. For each eigenvalue $\lambda_i(\mathcal{L}_j)$ of matrix $\mathcal{L}_j$, $\mathrm{Re}(\lambda_i(\mathcal{L}_j))$ returns its real component, and $\min \mathrm{Re}(\lambda_i(\mathcal{L}_j))$ represents the minimum value among the real parts of all eigenvalues of $\mathcal{L}_j$.

Given a constant matrix $\boldsymbol{D}_j$, the matrix–vector product $\boldsymbol{D}_j \boldsymbol{w}_j$ satisfies the following component-wise outer bound: $\boldsymbol{D}_j^+ \underline{\boldsymbol{w}}_j - \boldsymbol{D}_j^- \overline{\boldsymbol{w}}_j \le \boldsymbol{D}_j \boldsymbol{w}_j \le \boldsymbol{D}_j^+ \overline{\boldsymbol{w}}_j - \boldsymbol{D}_j^- \underline{\boldsymbol{w}}_j$.

2. Problem formulation

An actual CPS can be modeled as an integration of the physical layer network and the network layer network [17], including physical processes and signal transmission processes. The two networks are coordinated and coupled with each other [18]. Consider a network with N subsystems interconnected in a CPS. The kth subsystem is described by the pair ($P^{(k)}$, $W^{(k)}$), where $P^{(k)}$ corresponds to the physical part, while $W^{(k)}$, $k \in \{1, \ldots, N\}$ denotes the cyber part.

In the physical layer, each subsystem is equipped with a set of sensors to measure part or all of the state variables. The sensor output $y_k = \bar{C} x_k$ plays a dual role: On one hand, it is used for communication among subsystems in the physical layer based on a specific network topology $\mathcal{H}$; on the other hand, it is transmitted to the cyber layer, enabling the latter to monitor and control the physical layer network.

The physical part $P^{(k)}$ is modeled by a nonlinear dynamical subsystem, denoted by $\sum^{(k)}$ [19]:

$$\sum^{(k)}: \quad \dot{x}_k(t) = \bar{A} x_k(t) + \bar{B} u_k(t) + \bar{D} \Phi_k(x, t) + \bar{E} \omega_k(t) - \alpha \sum_{r=1}^{N} h_{kr} \Lambda y_r(t), \tag{1}$$

where $x_k(t) \in \mathbb{R}^n$ is the state, $u_k(t) \in \mathbb{R}^e$ is the control input, $\omega_k(t) \in \mathbb{R}^m$ is the unknown input, $y_k(t) \in \mathbb{R}^p$ is the measurement output, and $\Phi_k(x, t) \in \mathbb{R}^r$ stands for the nonlinear term of the system. $\bar{A}, \bar{B}, \bar{C}, \bar{D}$, and $\bar{E}$ are matrices with appropriate dimensions. $\mathcal{H} = [h_{kr}] \in \mathbb{R}^{N\times N}$ and $\Lambda \in \mathbb{R}^{n\times p}$ are the coupling matrices describing the connections among components, and the fixed scalar α represents the coupling strength.

In order to facilitate the subsequent analysis with process noise and measurement noise, we integrate the above coupling subsystem model into a global continuous-time CPS model:

$$\begin{cases} \dot{x}(t) = Ax(t) + Bu(t) + Dw(t), \\ y_i(t) = Cx(t) + Fv(t), i = 1, 2, \ldots, m, \end{cases} \tag{2}$$

where $x(t) \in \mathbb{R}^n$, $u(t) \in \mathbb{R}^{n_u}$, $y(t) \in \mathbb{R}^{n_y}$, $w(t) \in \mathbb{R}^{n_w}$, and $v(t) \in \mathbb{R}^{n_v}$ stand for the state vector, the input vector, the output vector, the process noise vector, and the measurement noise vector, respectively. For all $t \geq 0$, satisfy $\underline{w} \leq w(t) \leq \overline{w}, \underline{v} \leq v(t) \leq \overline{v}$. The constant matrices A, B, D, C, and F are known a priori and have appropriate dimensions.

First, apply an equivalence transformation to the system matrix $A \in \mathbb{R}^{n\times n}$ to convert it into a block diagonal form [12]. Then there exists a nonsingular matrix $\Psi = [\Psi_1\ \Psi_2\ \cdots\ \Psi_s] \in \mathbb{R}^{n\times n}$, with each block $\Psi_j \in \mathbb{R}^{n\times n_j}$, satisfying the following relations: $A\Psi_j = \Psi_j A_j, A\Psi = \Psi\tilde{A}$. Here, $\tilde{A} = \mathrm{diag}\{A_j\}$, with $A_j \in \mathbb{R}^{n_j\times n_j}$. The dimensions of the blocks satisfy $\sum_{j=1}^{s} n_j = n$, and A_j is precisely the j-th diagonal block of $\tilde{A}$. The real block diagonal transformation of any A requires exact conditions and a given structure.

For the original system state $x(t) = \Psi\xi, \xi = [\xi_1^T\ \xi_2^T\ \ldots\ \xi_s^T]^T$, $\xi_j \in \mathbb{R}^{n_j}$, $\tilde{B} = \Psi^{-1}B, and\ \tilde{D} = \Psi^{-1}D$, the system (2) can be transformed into

$$\begin{cases} \dot{\xi}(t) = \tilde{A}\xi(t) + \tilde{B}u(t) + \tilde{D}w(t), \\ y_i(t) = C_i\xi(t) + F_i v(t), i = 1, 2, \ldots, m. \end{cases} \tag{3}$$

We have the following assumptions:

Assumption 1. [20] The pair (A, C) is observable, while (A, C_i) is unobservable for all $i \in \mathcal{V}$.

Assumption 2. [20] For $\forall i \in \mathcal{V},\ j \in \mathcal{S}$, the necessary condition for a matrix pair (A_j, C_{ij}) to be observable is that $C_{ij} \neq 0$.

Define $O_i \triangleq \{j \in \mathcal{S} \mid C_{ij} \neq 0\}$, and the corresponding unobservable set is the complement of O_i: $\overline{O}_i = \{j \in \mathcal{S} \mid j \notin O_i\}$. For any substate index $j \in \mathcal{S}$, its converse observable set is defined as $U_j \triangleq \{i \in \mathcal{V} \mid j \in O_i\}$, which collects all agents capable of observing substate ξ_j. The corresponding converse unobservable set reads $\overline{U}_j = \{i \in \mathcal{V} \mid j \notin O_i\}$. Thus we can get $i \in U_j \iff j \in O_i$; $i \in \overline{U}_j \iff j \in \overline{O}_i$.

Lemma 1. Different from the centralized observer scheme that relies on the single global observability of the pair (A, C), the distributed framework only requires the joint observability of all local output aggregations, where some individual pairs (A_j, C_{ij}) are unobservable and complete the estimation of the global system state through neighbor communication [4].

Assumption 3. [20] The system (3) is globally observable with $\bigcup_{j=1}^{s} O_j = \mathcal{S}$.

Assumption 4. [20] For a given communication topology graph $\mathcal{G}$, for $\forall j$, the nodes of set U_j and set $\overline{U}_j$ form subgraphs $\mathcal{G}_j$ and $\overline{\mathcal{G}}_j$, respectively. The nodes of the unobservable subgraph $\overline{\mathcal{G}}_j$ form a directed spanning tree, and the root node of the tree is pinned to the output edge of the observable subgraph $\mathcal{G}_j$.

It shows from Assumption 2 that for any $i \in \mathcal{V}$, there exists a nonsingular matrix ϑ_i such that system (4) has the following form:

$$\begin{cases}\dot{\xi}_{io}(t) = \tilde{A}_{io}\xi_{io}(t) + \tilde{B}_{io}u(t) + \tilde{D}_{io}w(t),\\ \dot{\xi}_j(t) = \tilde{A}_j\xi_j(t) + \tilde{B}_ju(t) + \tilde{D}_jw_j(t),\ j \in \overline{O}_i,\\ y_i(t) = C_{io}\xi_{io}(t) + F_{io}v(t),\ i = 1, 2, \ldots, m,\end{cases} \tag{4}$$

where

$$\vartheta_i\tilde{A}\vartheta_i^\top = \begin{bmatrix} A_{io} & \\ & A_{i\overline{o}}\end{bmatrix},\quad \vartheta_i\tilde{B} = \begin{bmatrix} B_{io}\\ B_{i\overline{o}}\end{bmatrix},\quad \tilde{C}\vartheta_i^\top = \begin{bmatrix} C_{io} & \mathbf{0}\end{bmatrix},\quad \vartheta_i\tilde{D} = \begin{bmatrix} D_{io}\\ D_{i\overline{o}}\end{bmatrix}.$$

Therefore, system (3) is virtually expressed as the form of system (4), which includes the observable subsystem and unobservable subsystem.

3. Main results

For $i \in \mathcal{V}$, $\underline{x}_i$ and $\overline{x}_i$ are the lower and upper bounds of the estimated state of the original system generated by the i observer, respectively. Define the error variables $e_{io}(t) = \xi_{io}(t) - \hat{\xi}_{io}(t)$, $e_{ioz}(t) = T_{io}\xi_{io}(t) - q_{io}(t)$, $\overline{e}_{ij}(t) = \overline{\xi}_{ij}(t) - \xi_j(t)$, and $\underline{e}_{ij}(t) = \xi_j(t) - \underline{\xi}_{ij}(t)$. The DIO of system (4) is designed as follows:

$$\begin{cases}\dot{q}_{io}(t) = T_{io}A_{io}\hat{\xi}_{io}(t) + T_{io}B_{io}u(t) + L_{io}\left(y_i(t) - C_{io}\hat{\xi}_{io}(t)\right),\\ \hat{\xi}_{io}(t) = q_{io}(t) + N_iy_i(t),\\ \overline{\xi}_{io}(t) = \hat{\xi}_{io}(t) + \overline{e}_{io}(t),\\ \underline{\xi}_{io}(t) = \hat{\xi}_{io}(t) + \underline{e}_{io}(t),\\ \dot{\overline{\xi}}_{ij} = \left(\mathcal{D}_{A_j} + \mathcal{F}_{A_j}^+\right)\overline{\xi}_{ij} - \mathcal{F}_{A_j}^-\underline{\xi}_{ij} + D_j^+\overline{w}_j(t) - D_j^-\underline{w}_j(t) + \gamma_j\sum_{k\in N_j}a_{ik}\left(\overline{\xi}_{kj} - \overline{\xi}_{ij}\right) + B_ju(t),\ j \in \overline{O}_i,\\ \dot{\underline{\xi}}_{ij} = \left(\mathcal{D}_{A_j} + \mathcal{F}_{A_j}^+\right)\underline{\xi}_{ij} - \mathcal{F}_{A_j}^-\overline{\xi}_{ij} + D_j^+\underline{w}_j(t) - D_j^-\overline{w}_j(t) + \gamma_j\sum_{k\in N_j}a_{ik}\left(\underline{\xi}_{kj} - \underline{\xi}_{ij}\right) + B_ju(t),\ j \in \overline{O}_i,\\ \overline{x}_i(t) = \Psi^+\overline{\xi}_i(t) - \Psi^-\underline{\xi}_i(t),\\ \underline{x}_i(t) = \Psi^+\underline{\xi}_i(t) - \Psi^-\overline{\xi}_i(t),\end{cases} \tag{5}$$

where γ_j is a scalar to be designed, L_{io} and N_i are matrices to be designed, and the transformation matrix is defined as $T_{io} = I - N_iC_{io}$, $\overline{e}_{io}(t) = \overline{\xi}_{io}(t) - \hat{\xi}_{io}(t)$, and $\underline{e}_{io}(t) = \underline{\xi}_{io}(t) - \hat{\xi}_{io}(t)$.

The following theorem provides the parameter design strategy and stability demonstration for the observation error system.

Theorem 1. Under the assumption that 1–4 holds, for $\forall i \in \mathcal{V}$, if there is $\underline{x}_i(0) \le x(0) \le \overline{x}_i(0)$ at the initial time and the following conditions are satisfied, then for all $t > 0$, the estimators $\overline{x}_i(t)$ and $\underline{x}_i(t)$ in system (5) satisfy $\underline{x}_i(t) \le x(t) \le \overline{x}_i(t)$.

(i) There exist matrices T_{io} and L_{io}, such that $M_{io} = (T_{io}A_{io} - L_{io}C_{io})$ is a Hurwitz matrix.
(ii) For $\forall j \in \mathcal{S}$, there exists $\varepsilon_j > 0$ and positive definite symmetric matrix Q_j, P_j such that

$$(A_j^{\mathcal{M}})^TP_j + P_jA_j^{\mathcal{M}} + Q_j \le \varepsilon_jP_j. \tag{6}$$

(iii) Let $\gamma_j > 0$, $j \in \mathcal{S}$ satisfy

$$\gamma_j \ge \frac{\varepsilon_j}{2\min\mathrm{Re}\left(\lambda_i(\mathcal{L}_j)\right)}, \tag{7}$$

where $\mathcal{L}_j$ denotes the submatrix of the Laplacian matrix $\mathcal{L}$ [12] and removes rows h and columns $h \in U_j$ from $\mathcal{L}$.

Proof. Its dynamic satisfies

$$\begin{aligned}\dot{e}_{ioz}(t) &= M_{io}e_{io}(t) + H_{io}d(t),\\ e_{io}(t) &= e_{ioz}(t) + K_{io}d(t).\end{aligned} \tag{8}$$

For each i, where $H_{io} = (T_{io}D_{io} - (M_{io}N_i + L_{io})F_{io})$, $K_{io} = (I - N_iF_{io})$, and $d_i(t) = \begin{pmatrix} w_i(t) \\ v_i(t) \end{pmatrix}$, deduce the error dynamics of $e_{io}(t)$ as shown below:

$$\dot{e}_{ioz}(t) = M_{io}e_{ioz}(t) + H_{io}d(t). \tag{9}$$

Further, the expression of the estimation error is

$$e_{io}(t) = e_{ioz}(t) + K_{io}d(t). \tag{10}$$

Therefore, for all $t \geq 0$, the outer bound of the estimation error satisfies

$$\begin{aligned}\overline{e}_{ioz}(t) &= \Psi^{+}_{M_{io},H_{io}}(t)\overline{d} - \Psi^{-}_{M_{io},H_{io}}(t)\underline{d} + \Psi^{+}_{M_{io}}(t)\overline{e}_{ioz}(0) - \Psi^{-}_{M_{io}}(t)\underline{e}_{ioz}(0),\\ \underline{e}_{ioz}(t) &= \Psi^{+}_{M_{io},H_{io}}(t)\underline{d} - \Psi^{-}_{M_{io},H_{io}}(t)\overline{d} + \Psi^{+}_{M_{io}}(t)\underline{e}_{ioz}(0) - \Psi^{-}_{M_{io}}(t)\overline{e}_{ioz}(0).\end{aligned} \tag{11}$$

Finally, the upper and lower bounds of error are obtained:

$$\begin{cases}\overline{e}_{io}(t) = \overline{e}_{ioz}(t) + K^{+}_{io}\overline{d} - K^{-}_{io}\underline{d},\\ \underline{e}_{io}(t) = \underline{e}_{ioz}(t) + K^{+}_{io}\underline{d} - K^{-}_{io}\overline{d}.\end{cases} \tag{12}$$

By comdtion (i), $M_{io}$is a Hurwitz matrix. Then error dynamic system (9) is bounded and stable. Therefore, $e_{io} \in [\underline{e}_{io}, \ \overline{e}_{io}]$. Note that by formula (5), we have $\underline{\xi}_{io}(t) \leq \xi_{io}(t) \leq \overline{\xi}_{io}(t)$.

For any j, define error $\overline{e}_{ij}(t) = \overline{\xi}_{ij}(t) - \xi_j(t)$, $\underline{e}_{ij}(t) = \xi_j(t) - \underline{\xi}_{ij}(t)$, then the dynamic error satisfies

$$\begin{aligned}\dot{\overline{e}}_{ij}(t) &= (\mathcal{D}_{A_j} + \mathcal{F}^{+}_{A_j})\overline{\xi}_{ij}(t) - \mathcal{F}^{-}_{A_j}\underline{\xi}_{ij}(t) + \gamma_j \sum_{k\in N_i} a_{ik}(\overline{\xi}_{kj}(t) - \overline{\xi}_{ij}(t))\\ &\quad + B_ju(t) + D^{+}_j\overline{w}_j(t) - D^{-}_j\underline{w}_j(t) - A_j\xi_j(t) - B_ju(t) - D_jw_j(t)\\ &= (\mathcal{D}_{A_j} + \mathcal{F}^{+}_{A_j})\overline{e}_{ij}(t) + \mathcal{F}^{-}_{A_j}\underline{e}_{ij}(t) + \gamma_j \left[\sum_{k\in\overline{U}_j} a_{ik}\overline{e}_{kj} - \sum_{k\in N_i} a_{ik}\overline{e}_{ij}\right]\\ &\quad + \gamma_j \sum_{k\in U_j} a_{ik}\overline{e}_{kj} + D^{+}_j\overline{w}_j(t) - D^{-}_j\underline{w}_j(t) - D_jw_j(t).\end{aligned} \tag{13}$$

Similarly, we have

$$\begin{aligned}\dot{\underline{e}}_{ij}(t) &= (\mathcal{D}_{A_j} + \mathcal{F}^{+}_{A_j})\underline{e}_{ij}(t) + \mathcal{F}^{-}_{A_j}\overline{e}_{ij}(t) + \gamma_j \left[\sum_{k\in\overline{U}_j} a_{ik}\underline{e}_{kj} - \sum_{k\in N_i} a_{ik}\underline{e}_{ij}\right]\\ &\quad + \gamma_j \sum_{k\in U_j} a_{ik}\underline{e}_{kj} + D_jw_j(t) - (D^{+}_j\underline{w}_j(t) - D^{-}_j\overline{w}_j(t)).\end{aligned} \tag{14}$$

For a fixed index j, let the vectors $\overline{e}_{\overline{u}j} \in \mathbb{R}^{n_j|\overline{U}_j|}$ and $\overline{e}_{uj} \in \mathbb{R}^{n_j|U_j|}$ be defined as the stacked vectors of all $\bar{e}_{ij}$ satisfying $i \in \bar{U}_j$ and $i \in U_j$, respectively. Similarly, define $\underline{e}_{\overline{u}j} \in \mathbb{R}^{n_j|\overline{U}_j|}$ and $\underline{e}_{uj} \in \mathbb{R}^{n_j|U_j|}$. To facilitate the subsequent analysis, construct the error vector $\overline{e}_j = \begin{bmatrix} \overline{e}_{uj} \\ \overline{e}_{\overline{u}j} \end{bmatrix} \in \mathbb{R}^{n_j m}, i \in \mathcal{V}$. Let $\overline{w}_{ij} = \gamma_j \sum_{k \in U_j} a_{ik} \overline{e}_{kj}$, $i \in U_j$. The symbol $\overline{w}_j(t)$ holds for every $i \in U_j$. Denote by $\overline{w}_j(t)$ the vector obtained by stacking all $\overline{w}_{ij}$ with $i \in \overline{U}_j$. Then $\overline{w}_j(t) = W_j \overline{e}_{uj}$, where the matrix is $W_j \in \mathbb{R}^{n_j|\overline{U}_j| \times n_j|\overline{U}_j|}$.

Therefore, the error dynamics can be expressed as

$$\begin{bmatrix} \dot{\overline{e}}_{\overline{u}j} \\ \dot{\underline{e}}_{\overline{u}j} \end{bmatrix} = \Xi_{ej} \begin{pmatrix} \overline{e}_{\overline{u}j} \\ \underline{e}_{\overline{u}j} \end{pmatrix} + \begin{pmatrix} I \otimes [(D_j^+ \overline{w}_j(t) - D_j^- \underline{w}_j(t)) - D_j w_j(t)] \\ I \otimes [D_j w_j(t) - (D_j^+ \underline{w}_j(t) - D_j^- \overline{w}_j(t))] \end{pmatrix} + \begin{bmatrix} W_j & \\ & W_j \end{bmatrix} \begin{pmatrix} \overline{e}_{uj} \\ \underline{e}_{uj} \end{pmatrix}, \tag{15}$$

where

$$\Xi_{ej} = \begin{pmatrix} I \otimes (\mathcal{D}_{A_j} + \mathcal{F}_{A_j}^+) - \gamma_j \mathcal{L}_j \otimes I & I \otimes \mathcal{F}_{A_j}^- \\ I \otimes \mathcal{F}_{A_j}^- & I \otimes (\mathcal{D}_{A_j} + \mathcal{F}_{A_j}^+) - \gamma_j \mathcal{L}_j \otimes I \end{pmatrix}.$$

e_{io} is bounded and positive, and the vectors $\overline{e}_{uj} \in \mathbb{R}^{n_j|U_j|}$ and $\underline{e}_{uj} \in \mathbb{R}^{n_j|U_j|}$ are defined as the stacked vectors of all $\bar{e}_{ij}$ and $\underline{e}_{ij}$ satisfying $i \in U_j$, respectively. So the estimation errors $\overline{e}_{uj}$ and $\underline{e}_{uj}$ are bounded and positive, and also the disturbance interval width $\overline{w} - \underline{w}$ is a known bounded constant. Since $W_j = \gamma_j A_{\bar{U}_j U_j} \otimes I$ and $\gamma_j > 0$, the necessary and sufficient condition for the joint observation error $e_{\overline{u}j}$ to be positive and uniformly bounded is that the matrix Ξ_{ej} is a Hurwitz matrix and a Metzler matrix. Next, we prove that the matrix Ξ_{ej} is a Hurwitz matrix and a Metzler matrix, respectively:

Step 1: The off-diagonal elements of $I \otimes (\mathcal{D}_{Aj} + \mathcal{F}_{Aj}^+) - \gamma_j \mathcal{L}_j \otimes I$ are positive, all entries of $\mathcal{F}_{A_j}^+$ and $\mathcal{F}_{A_j}^-$ are nonnegative,and the matrix Ξ_{ej} is a Metzler matrix.

Step 2: From condition (ii), it follows from Lemma 7 in [21] that there necessarily exists for any $j \in \mathcal{S}$, $\varepsilon_j^1 > 0$, $\varepsilon_j^2 > 0$, and symmetric positive definite matrix $Q_j^1, Q_j^2, P_j^1, P_j^2$ such that

$$A_j^\top P_j^1 + P_j^1 A_j + Q_j^1 \leq \varepsilon_j^1 P_j^1, \tag{16}$$

and

$$(\mathcal{D}_{A_j} + \mathcal{F}_{A_j})^\top P_j^2 + P_j^2 (\mathcal{D}_{A_j} + \mathcal{F}_{A_j}) + Q_j^2 \leq \varepsilon_j^2 P_j^2. \tag{17}$$

Taking $\varepsilon_j = \max\{\varepsilon_j^1, \varepsilon_j^2\}$, we have $\varepsilon_j \geq \varepsilon_j^1$ and $\varepsilon_j \geq \varepsilon_j^2$ combined with the inequality of Eqs (16) and (17), thus the following inequalities hold:

$$(A_j - \gamma_j \lambda_{ji} I_j)^T P_j^1 + P_j^1 (A_j - \gamma_j \lambda_{jk} I) \leq \varepsilon_j P_j^1 - 2\gamma_j \lambda_{jk} P_j^1, \tag{18}$$

and

$$\left(\mathcal{D}_{A_j} + |\mathcal{F}_{A_j}| - \gamma_j \lambda_{ji} I\right)^T P_j^2 + P_j^2 \left(\mathcal{D}_{A_j} + |\mathcal{F}_{A_j}| - \gamma_j \lambda_{ji} I\right) \leq \varepsilon_j P_j^2 - 2\gamma_j \lambda_{jk} P_j^2. \tag{19}$$

Both $(A_j - \gamma_j \lambda_{ji} I)$ and $(\mathcal{D}_{A_j} + |\mathcal{F}_{A_j}| - \gamma_j \lambda_{ji} I)$ are Hurwitz matrices. Therefore, the matrix $\begin{bmatrix} A_j - \gamma_j \lambda_{ji} I & 0 \\ 0 & \mathcal{D}_{A_j} + |\mathcal{F}_{A_j}| - \gamma_j \lambda_{ji} I \end{bmatrix}$ is a Hurwitz matrix.

In summary, Ξ_{ej} is the Metzler-Hurwitz matrix. This means that $\underline{x}_i(t) \leq x_i(t) \leq \overline{x}_i(t), \ \forall i \in \mathcal{V}$. The proof is completed. □

Remark 2. When T_{io} is a identity matrix, $\dot{q}_{io}(t) = A_{io}\hat{\xi}_{io}(t) + B_{io}u(t) + L_{io}\left(y_i(t) - C_i\hat{\xi}_{io}(t)\right)$ is a traditional interval observer.

Algorithm 1 Design of DIO for CPS

- Compute the Laplacian matrix $\mathcal{L}$ of the communication topology.
- Compute the nonsingular similarity matrix $\Psi = [\Psi_1 \ \Psi_2 \ \cdots \ \Psi_s] \in \mathbb{R}^{n\times n}$ from the generalized eigenvectors of A satisfying $A\Psi = \Psi\tilde{A}$. Calculate $\Psi^+ = \max(\Psi, 0)$, $\Psi^- = \max(-\Psi, 0)$; check the invertibility of Ψ as the feasibility condition.
- **for** each $j \in \mathcal{S}$ **do**
  - Compute A_j, C_j, B_j, D_j, $\mathcal{L}_j$, $\mathcal{D}_{A_j} + \mathcal{F}^+_{A_j}$ and $\mathcal{F}^-_{A_j}$.
  - Select parameters ε_j, P_j, Q_j in (6); choose γ_j in (7).
  - **for** each agent $i \in \mathcal{V}$ **do**
    - Construct non-singular transformation matrix ϑ_i; verify invertibility, reconstruct if singular.
    - Obtain A_{io}, C_{io}, B_{io}, D_{io} and compute observer gain L_{io}, auxiliary matrix N_i, and transformation matrix $T_{io} = I - N_iC_{io}$.
  - **end for**
  - **for** each $j \in \mathcal{S}$ **do**
    - Construct error dynamics and update state bounds.
  - **end for**
- **end for**

4. Numerical simulation

In this section, the effectiveness of the proposed DIO method is verified by a simple numerical simulation. Consider the following system: $A = \mathrm{diag}\{A_1, A_2, A_3, A_4\}$, where,

$$A_1 = \begin{bmatrix} -2.2 & -1.1 & -0.6 \\ 1.3 & -1.4 & 0.7 \\ 0.9 & 1.0 & -1.8 \end{bmatrix}, \quad A_2 = \begin{bmatrix} -1.5 & -1 & -0.5 \\ 1.5 & 1 & 0.5 \\ 1 & 1 & 0 \end{bmatrix}, \quad A_3 = \begin{bmatrix} -0.5 & 1.2 & 0 \\ -1.2 & -0.5 & 0 \\ 0 & 0 & -2 \end{bmatrix}, \quad A_4 = \begin{bmatrix} -4 & 1.8 & 0.6 \\ 2.5 & -5 & -1.2 \\ 1.0 & 0.8 & -6 \end{bmatrix}.$$

$$C = \begin{bmatrix} C_1 \\ C_2 \\ C_3 \\ C_4 \end{bmatrix} = \left[\begin{array}{cccccccccccc} 0 & 0 & 0 & 0 & 0 & 0 & -1 & -2 & 1 & 0 & 0 & 0 \\ 0 & 0 & 0 & 0 & 0 & 0 & 1 & 0 & 2 & 0 & 0 & 0 \\ \hline 0 & 0 & 0 & 0 & 0 & 0 & 0 & 0 & 0 & -1 & -2 & 1 \\ 0 & 0 & 0 & 0 & 0 & 0 & 0 & 0 & 0 & 1 & 0 & 2 \\ \hline 1.2 & -0.8 & 0.5 & 0 & 0 & 0 & 0 & 0 & 0 & 0 & 0 & 0 \\ 0.3 & 1.5 & -0.7 & 0 & 0 & 0 & 0 & 0 & 0 & 0 & 0 & 0 \\ \hline 0 & 0 & 0 & 1 & 0.9 & 0 & 0 & 0 & 0 & 0 & 0 & 0 \\ 0 & 0 & 0 & 0 & 1.1 & 1 & 0 & 0 & 0 & 0 & 0 & 0 \end{array}\right].$$

$$B = \begin{bmatrix} 1 & -1 & 1 & 1 & -1 & 1 & 1 & -1 & 1 & 1 & -1 & 1 \end{bmatrix}^T, \quad D = I_{12}, \quad F = I_8.$$

This system is excited by a periodic signal defined by $u(t) = 3\sin(t) - 2\sin(3t)$. On the other hand, its dynamics are subject to unknown but bounded state disturbances

$$\forall t \geq 0,\ \mathbf{w}(t) \in [\mathbf{w}] = \begin{pmatrix} [-0.5,\ 0.5] \\ [-0.5,\ 0.5] \\ [-0.5,\ 0.5] \\ [-0.5,\ 0.5] \end{pmatrix}, \tag{20}$$

and its measured output is corrupted by an additive bounded measurement noise,

$$\forall t \geq 0,\ \mathbf{v}(t) \in [\mathbf{v}] = \begin{pmatrix} [-0.2,\ 0.2] \\ [-0.2,\ 0.2] \\ [-0.2,\ 0.2] \\ [-0.2,\ 0.2] \end{pmatrix}. \tag{21}$$

Design observer (5) as examples, and the values of the obtained matrices L, N, and T are

$$L_{1o} = \begin{bmatrix} -0.1438 & 0.2192 \\ -0.1710 & 0.0097 \\ 0.1687 & -0.3754 \end{bmatrix}, \quad N_{1o} = \begin{bmatrix} 0.0121 & -0.0059 \\ 0.0080 & 0.0105 \\ 0.0020 & -0.0190 \end{bmatrix}, \quad T_{1o} = \begin{bmatrix} 1.0180 & 0.0242 & -0.0003 \\ -0.0025 & 1.0160 & -0.0290 \\ 0.0211 & 0.0041 & 1.0360 \end{bmatrix},$$

$$L_{2o} = \begin{bmatrix} -0.0199 & 0.0102 \\ -0.0116 & 0.0149 \\ -0.0093 & 0.0093 \end{bmatrix}, \quad N_{2o} = \begin{bmatrix} 0.0077 & 0.0003 \\ 0.0024 & 0.0134 \\ -0.0124 & 0.0077 \end{bmatrix}, \quad T_{2o} = \begin{bmatrix} 1.0074 & 0.0154 & -0.0083 \\ -0.0110 & 1.0048 & -0.0292 \\ -0.0202 & -0.0248 & 0.9969 \end{bmatrix},$$

$$L_{3o} = \begin{bmatrix} 0.7526 & -0.1598 \\ 0.1947 & 0.9015 \\ 0.3619 & 0.1655 \end{bmatrix}, \quad N_{3o} = \begin{bmatrix} 0121 & -0.0059 \\ 0.0080 & 0.0105 \\ 0.0020 & -0.019 \end{bmatrix}, \quad T_{3o} = \begin{bmatrix} 0.9859 & 0.0474 & -0.0243 \\ -0.0481 & 0.9987 & -0.0039 \\ -0.0055 & -0.0101 & 1.0044 \end{bmatrix},$$

$$L_{4o} = 10^{-7} \cdot \begin{bmatrix} -0.0649 & -0.3643 \\ 0.2479 & 0.5028 \\ 0.5653 & 0.5702 \end{bmatrix}, \quad N_{4o} = 10^{-4} \cdot \begin{bmatrix} 0.1924 & -0.1688 \\ -0.2713 & -0.1151 \\ -0.0566 & 0.0811 \end{bmatrix}, \quad T_{4o} = \begin{bmatrix} 1 & 0 & 0 \\ 0 & 1 & 0 \\ 0 & 0 & 1 \end{bmatrix}.$$

Therefore, $(\boldsymbol{A}, \boldsymbol{C})$ is an observable pair, but for $\forall i \in \mathcal{V}$, the local system $(\boldsymbol{A}, \boldsymbol{C}_i)$ is unobservable. After calculation, the matrix is observable for $(\boldsymbol{A}_1, \boldsymbol{C}_{31})$, $(\boldsymbol{A}_2, \boldsymbol{C}_{42})$, $(\boldsymbol{A}_3, \boldsymbol{C}_{13})$, and $(\boldsymbol{A}_4, \boldsymbol{C}_{24})$.

The set x is divided into four groups, and the following is obtained:

$$\mathcal{O}_1 = \{3\},\ \mathcal{O}_2 = \{4\},\ \mathcal{O}_3 = \{1\},\ \mathcal{O}_4 = \{2\}; \quad \mathcal{U}_1 = \{3\},\ \mathcal{U}_2 = \{4\},\ \mathcal{U}_3 = \{1\},\ \mathcal{U}_4 = \{2\}.$$

Both Assumptions 2 and 3 are satisfied.

The communication network of the four observers is given by the strongly connected directed graph in Figure 1, which obviously satisfies Assumption 4. Since $\mathcal{U}_2 = \{4\}$, the corresponding Laplacian matrix after deleting the corresponding rows and columns is:

$$\mathcal{L}_2 = \begin{bmatrix} 1 & -1 & 0 \\ 0 & 1 & -1 \\ -1 & 0 & 2 \end{bmatrix}.$$

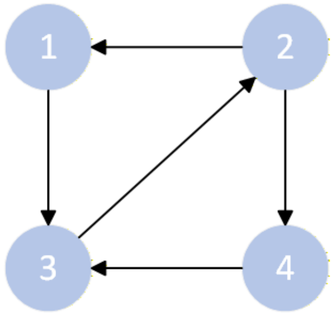

Figure 1. Communication topology.

The distributed observer form (6) is designed, and the initial value of the observer is given as follows: $\overline{\boldsymbol{x}}_{i0} = [3.5\ -4.5\ 2.5\ 3.5\ -4.5\ 2.5\ 3.5\ -4.5\ 2.5\ 3.5\ -4.5\ 2.5]^{\mathrm{T}}$, $\underline{\boldsymbol{x}}_{i0} = [6.5\ -1.5\ 5.5\ 6.5\ -1.5\ 5.5\ 6.5\ -1.5\ 5.5\ 6.5\ -1.5\ 5.5]^{\mathrm{T}}$, $i = 1, 2, 3, 4$. The symbols $\underline{x}_j^i$ and $\overline{x}_j^i$ denote the tracking of the j-th state component by the i-th observer.

Figures 2 and 3 show the tracking results of the DIO for state component 1 and state component 4, respectively. It shows in Figures 2 and 3 that the upper and lower bound trajectories generated by each observer always wrap the real state trajectory. Within one second, the state can be tracked, and the state is wrapped in the upper and lower bounds of the estimation interval, and thus the interval width is narrow, reflecting good estimation performance. In addition, Figure 4 shows the error norm variation curve of all observation systems. It can be seen that the error norm is always bounded and ultimately uniformly bounded.

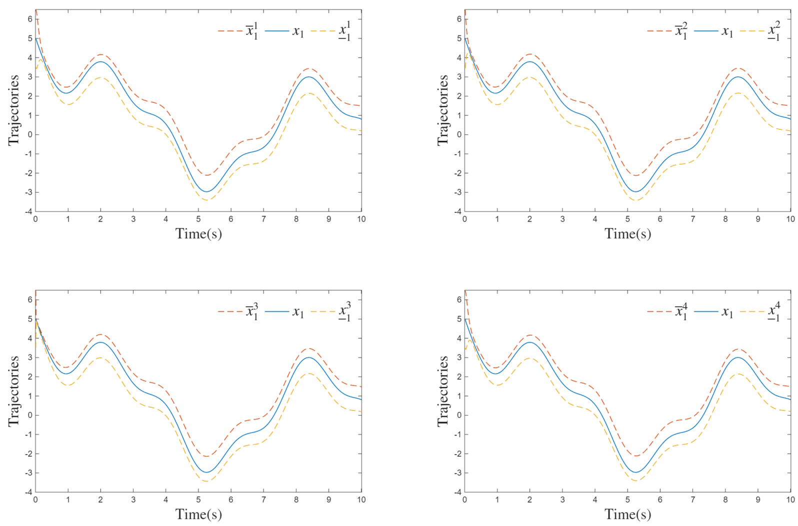

Figure 2. Tracking of the upper and lower bounds of the state estimate corresponding to state component 1 by each observer.

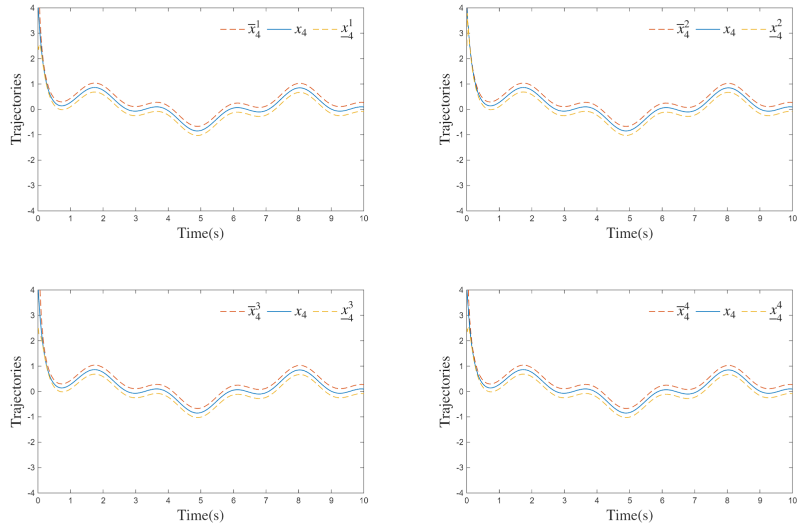

Figure 3. Tracking of the upper and lower bounds of the state estimate corresponding to state component 4 by each observer.

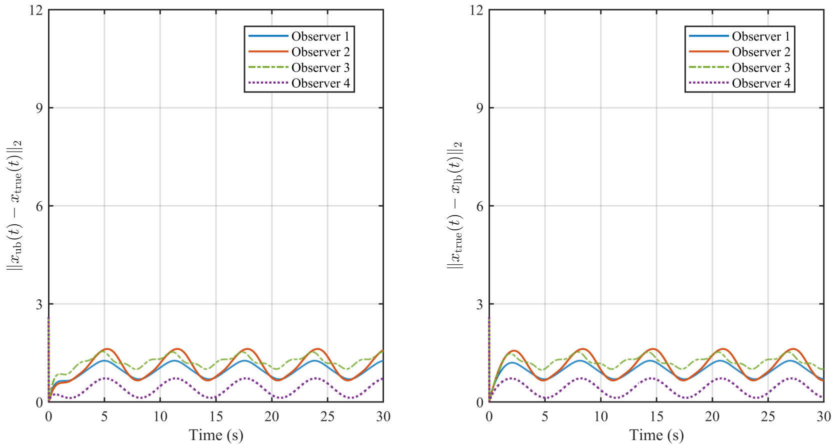

Figure 4. Comparison of the 2-norm errors among the upper bound, lower bound and true state of the interval observer. Left subplot: The 2-norm error $\|x_{\text{ub}}(t) - x_{\text{true}}(t)\|_2$ between the upper bound and the true state; right subplot: The 2-norm error $\|x_{\text{true}}(t) - x_{\text{lb}}(t)\|_2$ between the true state and the lower bound.

Suppose we consider another bounded noise and disturbance as follows:

$$\boldsymbol{w}(t) = 0.6\,(2\boldsymbol{r}_w - \mathbf{1}_3)\,, \quad \boldsymbol{r}_w \sim \mathcal{U}[0,1]^3,$$
$$\boldsymbol{v}(t) = 0.25\,(2\boldsymbol{r}_v - \mathbf{1}_2)\,, \quad \boldsymbol{r}_v \sim \mathcal{U}[0,1]^2,$$

where $\boldsymbol{r}_w$ and $\boldsymbol{r}_v$ are mutually independent random vectors, with each component uniformly distributed over $[0, 1]$. $\mathbf{1}_3$ and $\mathbf{1}_2$ denote the three-dimensional and two-dimensional all-one vectors, respectively.

The simulation results with revised bounded noise are illustrated in Figures 5 and 6. Therefore, under the conditions of Assumptions 1–4 and Theorem 1, the DIO is robust to any bounded noise and can ensure that the real state of the system is always within its interval estimation boundary.

As can be seen from Figure 7, although we have replaced the noise, its error norm is still within the interval broadband.

In order to more intuitively compare the differences in communication overhead between different methods, Table 1 summarizes the information dimensions that each method needs to exchange on each node. It can be seen that this paper effectively reduces the communication dimension.

Table 1. Comparison table of exchange information dimensions of nodes.

Method	Communication dimensions
Reference [22]	$D_i^{(1)} = 2 \cdot 4\aleph(N_i)n$
Reference [13]	$D_i^{(2)} = 2 \cdot 4\aleph(N_i)(n - n_o)$
Reference [12]	$D_i^{(3)} = 2 \cdot 4\aleph(N_i)(n - n_o)$
This paper	$D_i^{(4)} = 2 \cdot \aleph(N_i)(n - n_o)$

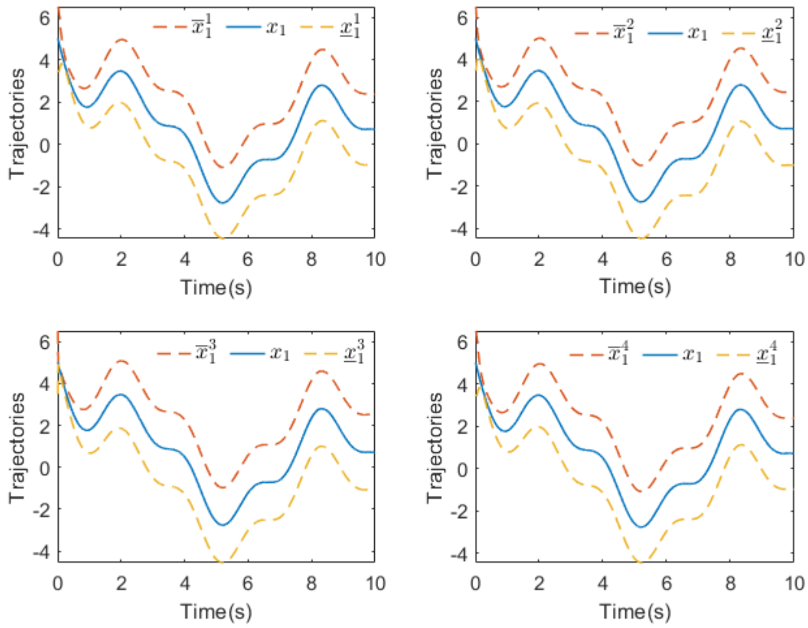

Figure 5. Tracking of the upper and lower bounds of the state estimate corresponding to state component 1 by each observer under modified noise settings.

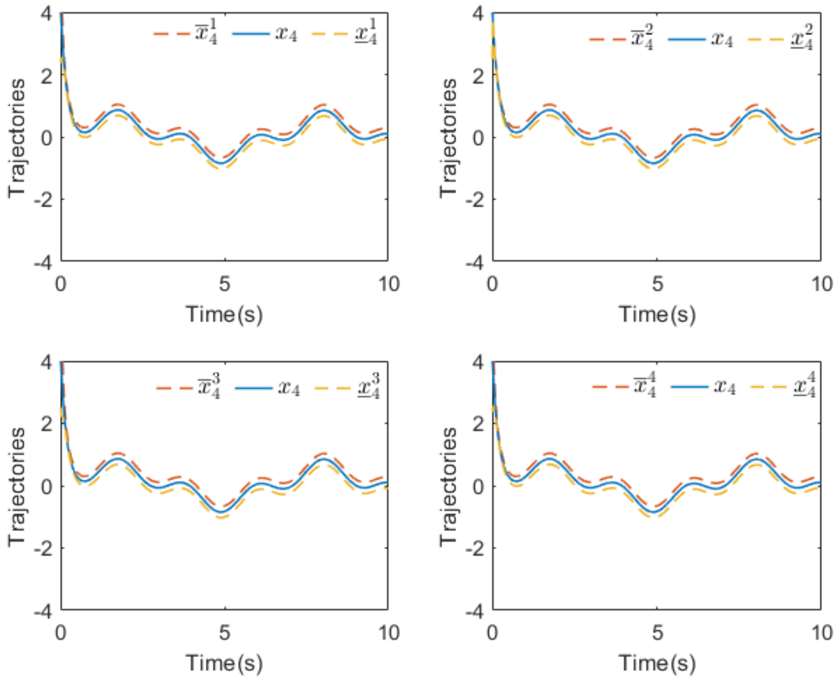

Figure 6. Tracking of the upper and lower bounds of the state estimate corresponding to state component 4 by each observer under modified noise settings.

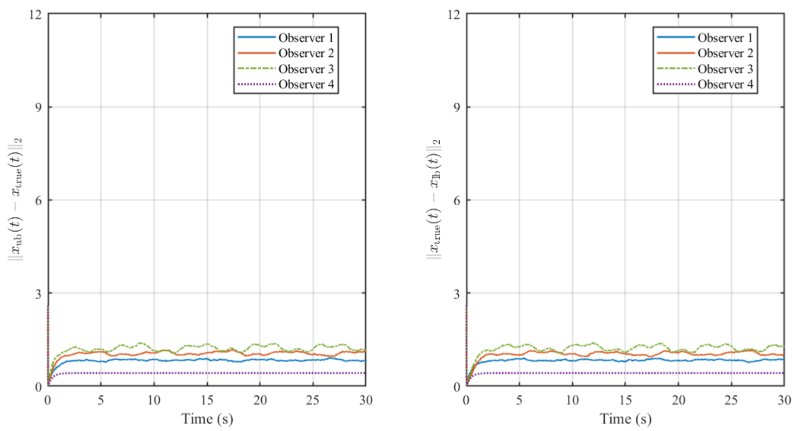

Figure 7. Comparison of the 2-norm errors among the upper bound, lower bound, and true state of the interval observer. Left subplot: The 2-norm error $\|x_{\text{ub}}(t) - x_{\text{true}}(t)\|_2$ between the upper bound and the true state; right subplot: The 2-norm error $\|x_{\text{true}}(t) - x_{\text{lb}}(t)\|_2$ between the true state and the lower bound under modified noise settings.

$\aleph(N_i)$ denotes the number of neighbors of node i, D_i represents the exchange information dimension of node i, and n is the dimension of the vector to be exchanged. Both References [12, 22] adopted the IPR method to design interval observers. Nevertheless, References [12, 13] only exchanged partial unknown information, which leads to the strict inequality $D_i^{(3)} = D_i^{(2)} < D_i^{(1)}$. Meanwhile, the proposed method abandons the IPR technique, so the dimension of information exchanged at each time is greatly reduced, $D_i^{(4)} < D_i^{(2)}$. Therefore, compared with the methods in References [12, 13, 22], less information needs to be exchanged in the proposed scheme.

5. Conclusions

In this paper, a state estimation method based on the DIO is proposed for a CPS system with disturbance and noise. This method simplifies the distributed collaborative design by system block diagonal transformation and gives a sufficient condition for the bounded stability of the observer error system by using the Lyapunov stability theory and Riccati equation. The simulation results show that the method can still achieve global state interval estimation, has a wide range of applications and less information exchange, which verifies the effectiveness of the scheme.

Author contributions

Danxia Li: Conceptualization, validation, methodology, writing – review & editing; Shan Wang: Conceptualization, validation, methodology, writing – review & editing; Yujie Chu: Validation, writing – original draft; Qian Shen: Validation, writing – original draft; Jiale Mi: Validation, writing – original draft; Zipeng Wang: Data analysis and manuscript revision. All authors confirm that they have read and approved the published version of the manuscript.

Use of Generative-AI tools declaration

The authors declare that they have not used Artificial Intelligence (AI) tools in the creation of this article.

Acknowledgments

This work was supported by Henan Province Science and Technology Research (252102210223), Henan Province University Key Scientific Research Project (24B413001), and Henan Province Humanities and Social Sciences General Project (2024-ZDJH-134).

Conflict of interest

The authors declare that they have no conflict of interest.

Zipeng Wang is an editorial board member for AIMS Mathematics and was not involved in the editorial review and/or the decision to publish this article.

References

1. S. J. Oks, M. Jalowski, M. Lechner, S. Mirschberger, M. Merklein, B. Vogel-Heuser, et al., Cyber-physical systems in the context of industry 4.0: A review, categorization and outlook, *Inform. Syst. Front.*, **26** (2024), 1731–1772. https://doi.org/10.1007/s10796-022-10252-x

2. D. Ding, Q. L. Han, Z. Wang, X. Ge, A survey on model-based distributed control and filtering for industrial cyber-physical systems, *IEEE T. Ind. Inform.*, **15** (2019), 2483–2499. https://doi.org/10.1109/TII.2019.2905295
3. L. Zhang, M. Lu, F. Deng, J. Chen, Cooperative output regulation subject to uncertain exosystems and its application: A fully distributed adaptive observer approach, *IEEE T. Control Netw. Syst.*, **12** (2025), 1830–1842. https://doi.org/10.1109/TCNS.2025.3543667
4. X. J. Zhang, K. Hengster-Movrić, M. Šebek, W. Desmet, C. Faria, Distributed observer and controller design for spatially interconnected systems, *IEEE T. Contr. Syst. T.*, **27** (2017), 1–13. https://doi.org/10.1109/TCST.2017.2769019
5. M. Long, H. Su, W. X. Zheng, Y. Wang, R. Su, Adaptive event-triggered distributed observer for unknown-input LTI systems, *IEEE T. Automat. Contr.*, **70** (2025), 8274–8281. https://doi.org/10.1109/TAC.2025.3581142
6. J. L. Gouzé, A. Rapaport, M. Z. Hadj-Sadok, Interval observers for uncertain biological systems, *Ecol. Model.*, **133** (2000), 45–56. https://dx.doi.org/10.1016/S0304-3800(00)00279-9
7. F. Mazenc, O. Bernard, Interval observers for linear time-invariant systems with disturbances, *Automatica*, **47** (2011), 140–147. https://doi.org/10.1016/j.automatica.2010.10.019
8. Z. H. Wang, Y. Shen, S. H. Guo, Interval observer design for linear descriptor systems, *Control Theory A.*, **35** (2018), 956–962. https://doi.org/10.7641/CTA.2017.70328
9. W. Zhu, Y. Zhou, M. Xiao, Interval observer design for linear discrete-time switched systems, *Microelectron. Comput.*, **40** (2023), 73–79. https://doi.org/10.19304/J.ISSN1000-7180.2022.0596
10. N. Meslem, Y. D. Ma, T. Raïssi, Z. H. Wang, New structure to design interval observers for linear continuous-time systems, *Int. J. Control*, **97** (2024), 1638–1646. https://doi.org/10.1080/00207179.2023.2221748
11. W. Y. Zhang, M. Z. Tang, S. H. Guo, Interval observer design for cyber-physical systems and application to attack detection, *J. Syst. Sci. Math. Sci.*, **41** (2021), 2379–2389. https://doi.org/10.12341/jssms20533
12. D. X. Li, J. Chang, W. S. Chen, T. Raïssi, IPR-based distributed interval observers design for uncertain LTI systems, *ISA T.*, **121** (2021), 147–155. https://doi.org/10.1016/J.ISATRA.2021.03.026
13. X. L. Wang, W. C. Xu, H. S. Su, Z. W. Gao, G. R. Chen, Designing a completely distributed interval observer for the LTI system, *IEEE T. Automat. Contr.*, **70** (2025), 1793–1808. https://doi.org/10.1109/TAC.2024.3471332
14. M. Khajenejad, S. Brown, S. Martínez, Distributed resilient interval observer synthesis for nonlinear discrete-time systems, *IEEE T. Automat. Contr.*, **70** (2025), 6656–6671. https://doi.org/10.1109/TAC.2025.3565189
15. D. X. Li, J. Chang, W. Chen, Event-triggered controller design for LTI systems: A distributed interval observer-based approach, *ISA T.*, **131** (2022), 146–159. https://doi.org/10.1016/J.ISATRA.2022.04.049
16. Z. H. Yin, J. Huang, T. N. Dinh, Design of distributed interval observers for multiple Euler–Lagrange systems, *Mathematics*, **11** (2023), 1872. https://doi.org/10.3390/math11081872

17. D. Xu, F. Zhu, Z. Zhou, Distributed fault detection and estimation in cyber-physical systems subject to actuator faults, *ISA T.*, **104** (2020), 162–174. https://doi.org/10.1016/j.isatra.2019.12.002
18. Y. Gao, W. Ren, R. Wu, Attack detection and security state estimation for cyber-physical systems, *Tsinghua Univ. (Nat. Sci. Edition)*, **61** (2021), 1234–1239. https://doi.org/10.16511/j.cnki.qhdxxb.2021.21.008
19. L. Ye, F. L. Zhu, J. Zhang, Sensor attack detection and isolation based on sliding mode observer for cyber-physical systems, *Int. J. Adapt. Control*, **34** (2020), 469–483. https://doi.org/10.1002/acs.3094
20. D. Li, J. Chang, W. S. Chen, J. Cieslak, *Distributed interval observer-based fault detection for a class of distributed measurement systems*, In: 2023 9th International Conference on Control, Automation and Robotics (ICCAR), **227–234** (2023). https://doi.org/10.1109/ICCAR57134.2023.10151712
21. F. Cacace, A. Germani, C. Manes, A new approach to design interval observers for linear systems, *IEEE T. Automat. Contr.*, **60** (2015), 1665–1670. https://doi.org/10.1109/TAC.2014.2364976
22. X. Wang, H. Su, F. Zhang, G. Chen, A robust distributed interval observer for LTI systems, *IEEE T. Automat. Contr.*, **68** (2023), 1337–1352. https://doi.org/10.1109/TAC.2022.3151586